Spatial Distribution of γ Emissivity and Fast Ions during (^3He)D ICRF Heating Experiments on JET

E Righi[1], D F H Start, C Warrick[2].

JET Joint Undertaking, Abingdon, Oxon, OX14 3EA.
[1] Imperial College of Science, Technology and Medicine, London, UK.
[2] AEA Technology, Culham, Oxfordshire, OX14 3DB, UK.

Introduction. During the 1991-92 JET experimental campaign the neutron profile monitors measured along both the horizontal and vertical lines of sight the γ emissivity produced by nuclear reactions of ^{3}He ions accelerated by ICRF heating with ^{9}Be impurities during ICRF heating experiments in a (^{3}He)D plasma [1]. In the present paper a numerical technique is presented that simulates such measurements by merging information obtained from the fast ion distribution and from nuclear reactions producing the observed γ emissivity. This technique is full of potentialities to be developed, and it can play an importat role in the identification of plasma instabilities that affect the redistribution of the fast ions in the plasma, like the TAE modes and the ripple in the tokamak magnetic field.

Production of γ photons during ^{3}He-^{9}Be reactions. High energy ^{3}He ions accelerated by ICRF heating can undergo exothermic nuclear reactions with ^{9}Be impurities present in the plasma, namely,

$$^9\text{Be}+^3\text{He}\rightarrow^{11}\text{B}+\text{p}+\gamma \qquad Q=10\ \text{MeV}, \tag{1}$$

$$^9\text{Be}+^3\text{He}\rightarrow^{11}\text{B}+\text{d}+\gamma \qquad Q=1.09\ \text{MeV} \tag{2}$$

$$^9\text{Be}+^3\text{He}\rightarrow^{11}\text{C}+\text{n}+\gamma \qquad Q=7.59\ \text{MeV}. \tag{3}$$

The γ photons are produced when the residual nucleus is formed in an excited state, and subsequently decays to one of the lower excited states, or the ground state. In the present analysis Eq.(1) is considered, because the reaction energy of Eq.(2) is one order of magnitude lower, and can therefore be neglected, while Eq.(3) is the isobaric equivalent of Eq.(1). Extensive studies of the ^{9}Be(^{3}He,p)^{11}B reaction exist [2,3,4,5,6], from which information can be obtained about the differential cross-sections at 90° in the laboratory frame of reference and in the energy range between 1 and 3 MeV for protons leaving ^{11}B in its excited states. Since the γ detectors used have no energy resolution, a "total" cross-section $(d\sigma / d\omega)_{tot}$ has been derived, sum of all the excitation curves for the energy levels from first to ninth, which gives an estimate of the relative probability that a γ photon is emitted from any excited state in the energy interval of interest (see Fig.1).

Simulation of γ-ray emission. In order to describe correctly the interation of ^{3}He ions with ^{9}Be impurities it is also necessary to know the distribution of ^{3}He ions in $(v_{\parallel}, v_{\perp}, r, \theta)$ space and the orbit paths of the fast ^{3}He ions. The distribution of ^{9}Be ions is here assumed to be uniform and with a concentration equal to 1% of the electron density, consistent with the measurements of Z_{eff} for the discharges considered. The ^3He distribution has been calculated by means of a 2D numerical code that solves the bounce-averaged steady-state Fokker-Planck equation in cylindrical coordinates [7]. This code does not include the effects of finite orbit width of high energy fast ions, which therefore have to be included *a posteriori*. To this end the orbit following code ORBIT [8] has been used that estimates the time $(\Delta t / T)_{T\to\infty}$ spent by the ^3He ions at each point in the configuration

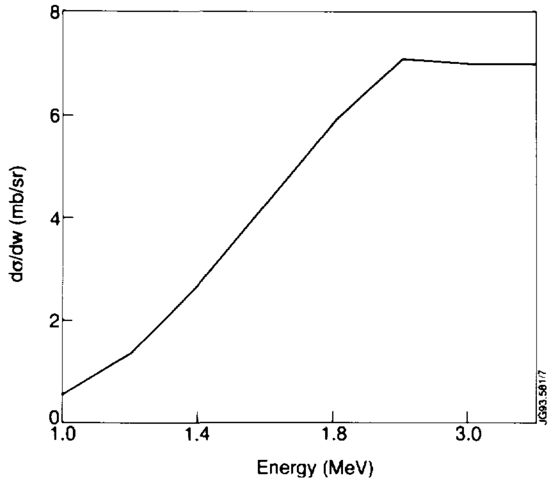

Fig.1. "Total" differential cross-section for ^{11}B.

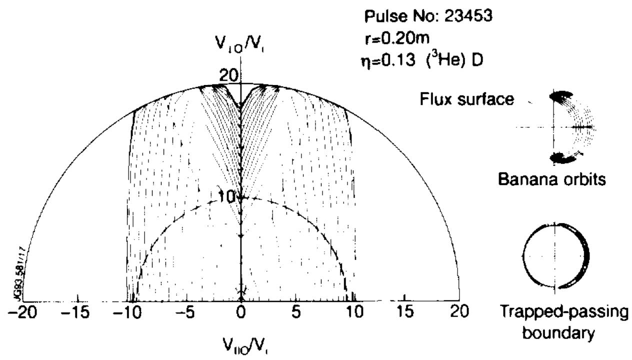

Fig.2. Minority ion distribution function in $(v_{||}, v_{\perp})$ space.

space. A plot of the intensity of γ emissivity,

$$I_\gamma \propto \int d^3r \int dE \sqrt{E} f(E,r,\theta) \left(\frac{d\sigma}{d\omega}\right)_{tot} \left(\frac{\Delta t}{T}\right)_{T\to\infty}, \tag{4}$$

can then be generated for each energy considered and a number of test particles, once the weight function,

$$w(E,r,\theta) = \sqrt{E} f(E,r,\theta) \left(\frac{d\sigma}{d\omega}\right)_{tot} \left(\frac{\Delta t}{T}\right)_{T\to\infty}, \tag{5}$$

is known. Information about the ^3He distribution in energy, pitch angle and minor radius and the excitation curves of ^{11}B have therefore been combined in the weight function Eq.(5) as input for the ORBIT code to calculate the γ-ray emission of monoenergetic test particles launched at the midplane. The results of simulations at different energies have been subsequently integrated to give the total γ emissivity.

Results and comparison with the experiment. The JET shots for which experimental measurements of the γ emissivity exist are those of Table I, where their main plasma parameters are listed. Measurements of γ emissivity can be plotted either as a 3D reconstruction of γ intensity in the poloidal plane, or as line integrated data of γ emission along a vertical and horizontal line of sight [1]. Both cases have been simulated numerically. In Fig.3 the intensity of γ emission in the (r,z) plane is reported for the off-axis discharge JPN 23450. Analysis of these simulations show that different types of orbits contribute to determine the two γ distributions when on-axis and off-axis ICRF are considered, which leads also to a different localization of the emissivity peak (the "hot spot"). In particular, the off-axis ICRF discharge (JPN 23450) is dominated by passing particles in the plasma centre, while trapped particles are localised either on the RF resonance or nearby. On the contrary, in the case of on-axis ICRF heating (JPN 23453) trapped particles dominate near the plasma centre (on the RF resonance), with a clear contribution of high energy D-shaped orbits. If the numerical γ emissivity in the (r,z) plane is line integrated into γ intensity along the horizontal and vertical lines of sight [1], then the γ-ray calculations can be compared with the experimental curves. The results, shown in Fig.4 for JPN 23450, clearly indicate that experiment and simulation agree qualitatively, meaning that the main elements responsible for the distribution of γ emissivity (and fast ions) are all present in the model. However the picture also shows that while along the horizontal line of sight the measured and calculated intensities have the same profiles, along the vertical line of sight the intensity peaks are displaced of one channel. This means that the simulated "hot spot" is displaced horizontally with respect to the measurement. This difference could find an explanantion in the approximations used. In particular, the Fokker-Planck code calculates f(E,r,θ) in cylindrical coordinates, while the actual discharges have substantial elongation and triangulation. Also orbit

Table I - Plasma parameters

	JPN 23450	JPN 23453
time slice (s)	49.0	49.0
plasma current (MA)	3.5	3.5
B_t on-axis (T)	3	3
T_{e0} (keV)	7.3	7.4
n_{e0} (10^{19} m^{-3})	2.8	3.0
P_{RF} (MW)	7.9	11.7
magnetic axis R_0 (m)	3.10	3.12
resonance off-set (m)	0.29	0.06
fast ion energy (MJ)*	0.2	1
Z_{eff}	1.5	1.6
n_{He}/n_{e0} *	0.045	0.13

**estimated with the orbit code PHANTOM [9] and cross-checked with experimental data*

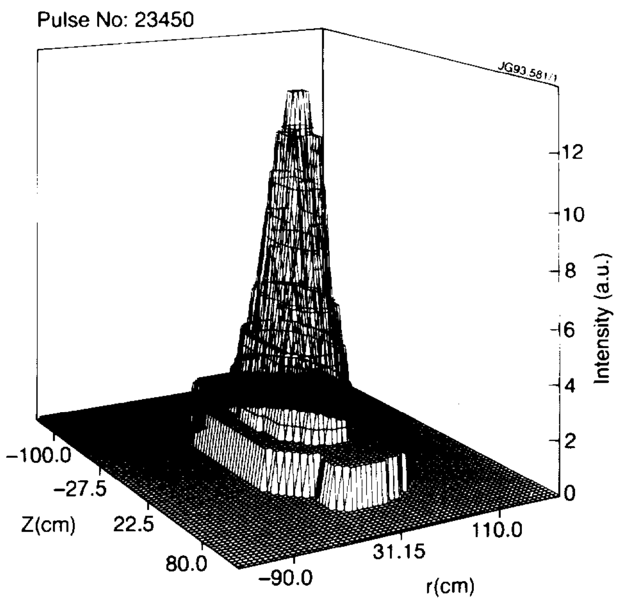

Fig.3. Numerical reconstruction of γ-ray emissivity in the poloidal plane for the off-axis ICRF heated discharge JPN 23450.

effects are not introduced self-consistently, but *a posteriori.* It is also not excluded that other nuclear reactions (of ^{12}C with ^{3}He, for instance) should be included in the analysis.

Conclusions and future work. In this paper a model has been presented that can simulate the γ emissivity in the poloidal cross-section during (^{3}He)D ICRF heated discharges in JET plasmas. Calculations show reasonable agreement with the experiment, indicating that all the main elements that produce the distribution are present. However the model is still only a first order description of the γ production. Future work will therefore be oriented especially to improve the calculation of the fast ion distribution function by including self-consistently effects of toroidal geometry and finite orbit widths of ^{3}He ions (through already available Monte-Carlo codes). This technique can be useful to analyse JET discharges in all those scenarios where the ^{3}He distribution plays a major role, like in the presence of Toroidal Alfven Eigenmode (TAE) modes or ripple in the tokamak magnetic field. In the former case the distribution is expected to lose its peakedness due to the redistribution of the passing fast ions into high energy D-shaped orbits.

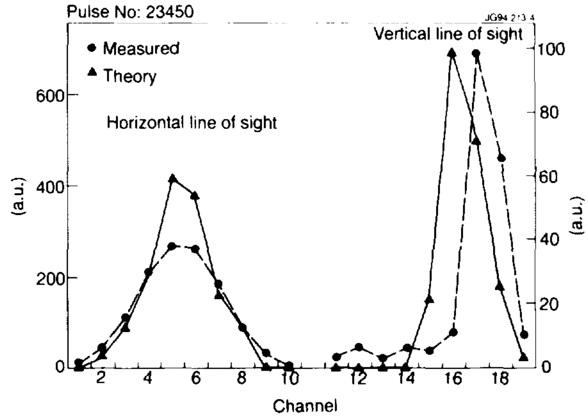

Fig.4. Comparison between experimental and theorietical line integrated intensity of γ emissivity along the horizontal and vertical lines of sight of the γ detectors for JPN 23450 (courtesy of P.J.A. Howarth).

Acknowledgements. The authors would like to acknowledge the cooperation with the JET RF Team and the Neutron Group, in particular P. van Belle, G. Sadler, P.J.A. Howarth and O.N. Jarvis. Special thanks go to Dr. E. Jelley, of the Nuclear Physics Laboratory in Oxford, for his precious help to dig out the references on ^{11}B cross-sections.

References

1. P.J.A. Howarth et al., these Proceedings.
2. H.D. Holmgren, M.L. Bullock and W.E. Kunz, Phys. Rev. **104** (1956), 1446.
3. S. Hinds and R. Middleton, Proc. Phys. Soc. **A74** (1959), 196.
4. E.A. Wolicki et al., Phys. Rev. **116** (1959), 1585.
5. S. Hinds and R. Middleton, Proc. Phys. Soc. **A75** (1960), 754.
6. W.R. Coker et al., Nucl. Physics **A91** (1967), 97.
7. M.R. O'Brien, M. Cox and D.F.H. Start, Nucl. Fusion **26** (1986), 1625.
8. P. van Belle, private communication.
9. E. Righi, Ph.D. thesis, Imperial College of Science, technology and Medicine (1994).